Inorganic Chemistry

pubs.acs.org/IC Article

Redox-Active Bis-Cyclometalated Iridium(III) Complex as a DNA Photo-Cleaving Agent

Justin Weynand, Angélica Moreno-Betancourt, Frédérique Loiseau, Nathalie Berthet, Eric Defrancq,* and Benjamin Elias*

Cite This: *Inorg. Chem.* 2020, 59, 2426−2433 Read Online

ACCESS | Metrics & More | Article Recommendations | Supporting Information

ABSTRACT: The development of new photoactive metal complexes that can trigger oxidative damages to the genetic material is of great interest. In the present paper, we describe the detailed study of a highly photo-oxidant iridium(III) complex that triggers photoinduced electron transfer (PET) with purine DNA bases. The PET has been studied by luminescence and laser flash photolysis experiments. From plasmid DNA agarose gel electrophoresis experiments, we demonstrated the high ability of the iridium complex to induce strand breaks upon light irradiation. Reactive oxygen species (ROS)-specific scavengers and stabilizers were employed to identify that the photocleavage process, the results of which infer singlet oxygen and hydrogen peroxide as the predominant species. To the best of our knowledge, the present work represents one of the few study for highly photo-oxidant bis-cyclometalated iridium(III) complex toward DNA.

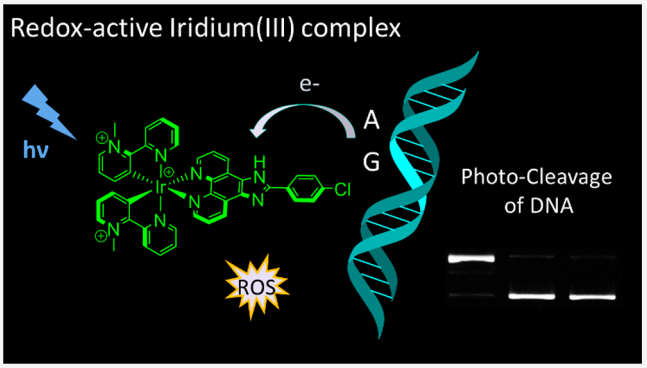

INTRODUCTION

The use of metal complexes in therapy have been the subject of much research. For example, platinum compounds, including the well-known cisplatin, have been extensively studied for cancer therapy.[1] However, researchers still try to overcome the problem of side effects arising with platinum compounds. There is continuous focus on the development of alternatives to platinum compounds with more specific actions.[2,3] In the context of photo dynamic therapy (PDT), ruthenium(II) complexes were found to be interesting thanks to their large Stoke's shift, absorption in the visible area, and ability to form singlet oxygen (type II photo-oxidation).[4,5] In addition to singlet oxygen photoproduction, some of these complexes have been shown to be highly oxidant under light irradiation.[6] These properties have been used to trigger oxidative electron transfer with DNA (type I photo-oxidation). For example, $[Ru(TAP)_3]^{2+}$ complex (TAP = 1,4,5,8-tetraazaphenanthrene) has been extensively studied by the group of Kirsch-De Mesmaeker.[7,8] In the presence of DNA, this complex is photoreduced by guanine nucleobase, leading to strand breaks and the formation of a photoadduct between the complex and guanine.[9] Such photoreactivity can be used to block the replication and transcription of DNA.[10] Therefore, these highly photo-oxidizing complexes constitute potential candidates in cancer therapy when type II photoreactivity (ROS photoproduction) is found unsuitable (e.g., hypoxia tumor). A dinuclear ruthenium(II) complex has also been reported recently to be highly phototoxic toward malignant human melanoma cells.[11] Unfortunately, despite their low toxicity in dark, polypyridyl ruthenium complexes have shown poor cell penetration and/or photostability (in particular with TAP ligands), limiting their use in clinical trials.[12−14]

More recently, Ir(III) complexes have emerged as promising PDT agents.[15−22] This is mainly due to their high luminescence quantum yields combined with their good photostability.[23,24] In addition, their photophysical and biological/chemical properties can be easily tuned. Some ruthenium(II), platinum(II), or iridium(III) complexes bearing 2-(4-chlorophenyl)-1*H*-imidazo[4,5-*f*][1,10]-phenanthroline (CPIP) ligand have been previously reported for selective G-quadruplex DNA recognition.[25−28] We have recently developed new Ir(III) complexes based on this CPIP.[25] Evidence for the formation of 8-oxo-dG by photoinduced electron transfer (PET) in G-rich sequences such as G-quadruplex DNA were provided. The interaction of these new iridium(III) complexes with G-quadruplex DNA was studied using various techniques (i.e., bio-layer interferometry, surface plasmon resonance, and CD melting experiments). Herein, in addition to our recent paper, we have extensively studied this PET between $[Ir(2,2'\text{-}C\hat{}N)_2CPIP]^{3+}$ (complex **1**,

Received: November 11, 2019
Published: January 24, 2020

https://dx.doi.org/10.1021/acs.inorgchem.9b03312
Inorg. Chem. 2020, 59, 2426−2433

Figure 1) with both guanine (G) and adenine (A) by electrochemical means, luminescence quenching with mono/

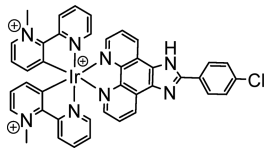

Figure 1. Structure of complex **1**: $[Ir(2,2'\text{-}C^{\wedge}N)_2CPIP]^{3+}$.

poly nucleotides, and time-resolved absorption spectroscopy. For the first time, the consequences (i.e., photodamages) of the high photo-oxidizing ability of the complex and the possible mechanisms involved in the photodamaging processes have been studied by agarose gel electrophoresis using pBR322 plasmid DNA.

RESULTS AND DISCUSSION

Photophysical Studies. Ir(III) complex **1** has been prepared as previously described.[25] It has been unambiguously characterized by ^{1}H NMR spectroscopy and high-resolution mass spectrometry (HRMS). The absorption spectrum in MeCN at room temperature (Figure 2 and Table 1) exhibits strong absorption bands in the UV region attributed to ligand centered (LC) transitions. The absorption bands at lower energy (λ > 340 nm) are assigned to charge transfer (CT) transitions. In the case of Ir(III) complexes, they usually correspond to a mixture of different charge transfer transitions (i.e., ligand to ligand, metal−ligand to ligand, and metal to ligand).[16,17] For complex **1**, they likely involve the metal and the C^N bpy-Me cyclometalated ligand in the HOMO−LUMO transitions. The luminescence spectra of complex **1** are poorly influenced by the solvent, in agreement with LC transitions (Figure 2 and Table 1). In contrast, at 77 K, the emission spectrum is blue-shifted, suggesting the contribution of a charge transfer process to the overall radiative deactivation process. The quantum yield and the luminescence lifetime of the complex are higher under argon in both organic and aqueous solvent, suggesting singlet oxygen photosensitization.

As described in our recent paper,[25] the oxidation and reduction potentials of complex **1** were determined by cyclic voltammetry measurements in dry deoxygenated acetonitrile. It displays a high oxidation power upon light irradiation (E^*_{red} = 1.59 V vs Ag/AgCl). Therefore, considering that E_{ox} of isolated G and A are close to +1.10 and +1.36 V vs Ag/AgCl, respectively,[29] a PET from these two nucleobases to the complex at the excited state could be possible. It was thus studied by luminescence quenching experiments (*vide infra*).

Luminescence Quenching Experiments with Mononucleotide dGMP and dAMP. Thanks to the ability of **1** to emit light in aqueous solvent, luminescence quenching experiments in the presence of DNA building blocks can be achieved. As previously described, the luminescence of complex **1** was quenched upon addition of increasing concentration of 2′-deoxyguanosine-5′-monophosphate (dGMP).[25] Interestingly, we also noticed that the addition of 2′-deoxyadenosine-5′-monophosphate (dAMP) also leads to a luminescence quenching, suggesting PET from the adenine to the excited complex (Figure 3). Considering the oxidation power of the excited state of **1** and using the empirical Rehm−Weller equation, it is expected that PET with G and A should be exergonic by about 0.55 and 0.29 eV, respectively.[30] Efficient luminescence quenching of the complex by G and A units is also in agreement with the high value of the dynamic quenching rate constant (k_q) obtained from the Stern−Volmer plots of **1** with dGMP and dAMP (Figure 3, $k_q = 2.26 \times 10^9$ M^{-1} s^{-1} and 3.20×10^8 M^{-1} s^{-1} for dGMP and dAMP, respectively), both close to the diffusion limit.

Luminescence Titration with GC- and AT-Containing Polynucleotides. In order to confirm the PET process with purine bases embedded in an oligonucleotide sequence, we performed the same luminescence quenching experiments with both GC- and AT-rich hairpins. We chose an GC- or AT-rich hairpin to confirm the PET with ODNs. First, we confirmed the formation of the hairpin structures in the buffer used (10 mM Tris-HCl, 50 mM NaCl, pH 7.4) using CD experiments (see Figure S1). In agreement with the PET observed with dGMP, the luminescence of the complex was quenched upon addition of GC hairpin oligonucleotide (Figure 4, purple line).

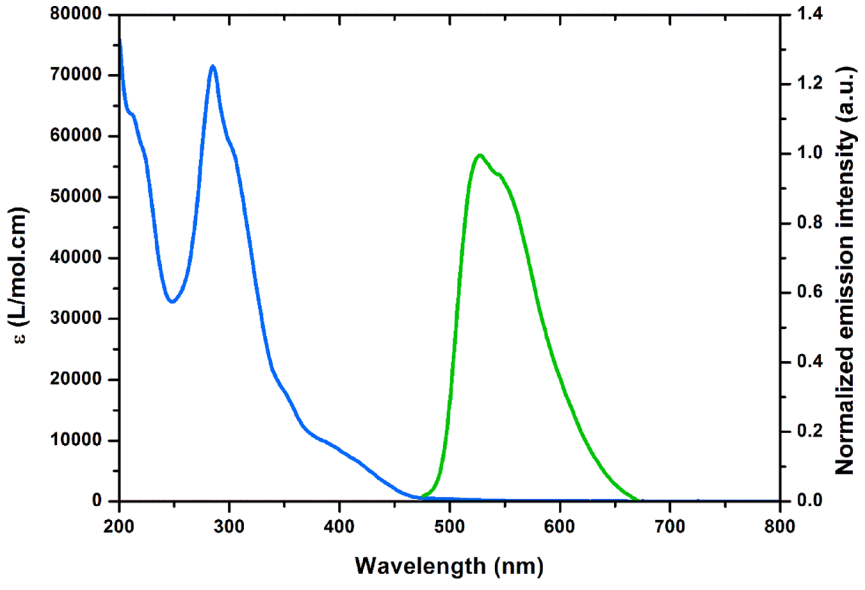

Figure 2. Absorption and emission spectra of **1** in MeCN at room temperature.

https://dx.doi.org/10.1021/acs.inorgchem.9b03312
Inorg. Chem. 2020, 59, 2426−2433

Table 1. Absorption and Luminescence Data of 1

	λ_{Abs} (ε)[a]	λ_{Em}[b]			Φ_{Em}[c]		τ (ns)[d]	
complex	MeCN	MeCN	H_2O	77 K	MeCN	H_2O	MeCN	H_2O
1	417 (6400)	528	528	504, 544	0.067 (0.136)	0.0018 (0.0018)	613 (950)	316 (560)

[a]λ in nm for the most bathochromic transition in MeCN with extinction coefficient ε (M^{-1} cm^{-1}, in brackets). [b]λ in nm at RT in MeCN, H_2O and at 77 K in EtOH/MeOH (4/1, v/v). [c]Luminescence quantum yields with excitation at λ_{exc} = 450 nm were determined under air (and argon in parentheses) by comparison with $[Ru(bpy)_3]^{2+}$. Errors are estimated to 10%. [d]Luminescence lifetimes (λ_{exc} = 405 nm, errors estimated to 5%) were measured under air (and argon in parentheses).

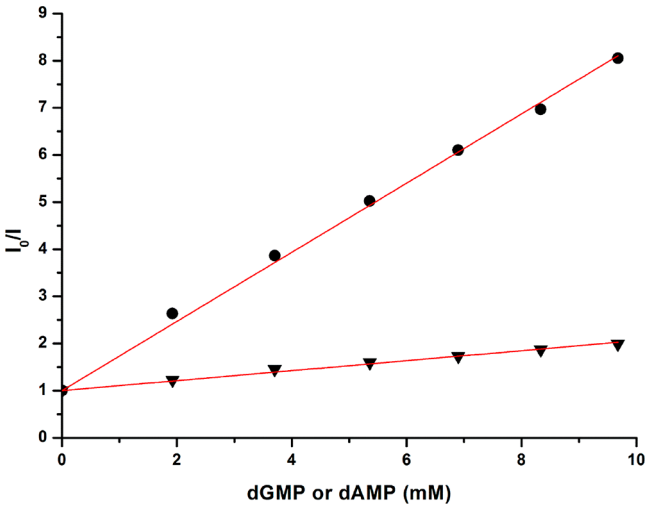

Figure 3. Stern–Volmer plots obtained upon the addition of dGMP (round) or dAMP (triangle) (0–10 mM) to **1** (50 μM, λ_{exc} = 350 nm). Measurements were carried out in 10 mM Tris-HCl (pH 7.4), under ambient air conditions.

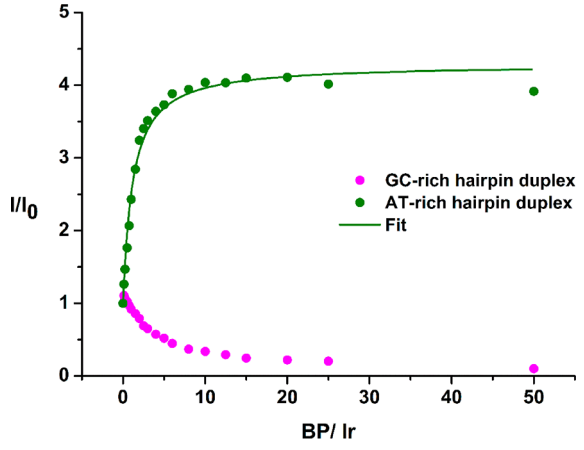

Figure 4. Steady-state luminescence titration of **1** (5 μM, λ_{exc} = 350 nm) with GC-rich hairpin duplex (in purple, 3′-$(GC)_4$TTTT$(GC)_4$-5′) and AT-rich hairpin duplex (in green, 3′-$(AT)_4$CCCC$(AT)_4$-5′). Measurements were performed using 5 μM of the complex in 10 mM Tris-HCl and 50 mM NaCl (pH 7.4) buffer under ambient air conditions.

Unexpectedly, the experiments with AT-rich hairpin duplex afforded strongly different results. Indeed, we observed a luminescence increase of complex **1** upon addition of AT-rich hairpin (Figure 4, green line). Two antagonist processes could occur when complex **1** interacts with AT-rich hairpin DNA: (i) a protection of the complex from the solvent and from oxygen by the DNA hydrophobic environment, leading to a luminescence increase, and (ii) a quenching by the adenine bases (as in the case of dAMP), resulting in a luminescence decrease. In this case, the protection effect should be predominant leading to a luminescence enhancement. This behavior is in accordance with the increased quantum yield and luminescence lifetime from (i) water to acetonitrile and (ii) air to argon. Indeed, the hydrophobic DNA microenvironment can be roughly assimilated to an acetonitrile medium. Binding affinity for AT-rich hairpin could be estimated by fitting the variation of the luminescence intensity as a function of the base-pair concentration. Complex **1** showed an apparent dissociation constant (K_D) of 44 μM. As the quenching process with GC-rich hairpin alters the luminescence of complex **1**, we used biolayer interferometry (BLI) to measure a K_D of 34 μM.[25]

Transient Species Formed by Flash Photolysis. To gain further insight into the PET, nanosecond time-resolved transient absorption measurements with complex **1** in the absence and presence of mononucleotides dGMP or dAMP were performed. All experiments were carried out in aqueous buffer and under argon. Figure 5A displays the transient absorption spectra of complex **1** recorded from 0 to 2700 ns in the absence of nucleobase. A bleaching around 390 nm, concomitant with two transient absorptions centered around 340–350 nm and 430–470 nm, are observed and are attributed to the presence of mixed CT excited states as previously described in the literature.[31] These transients decay in 980 ns according to monomolecular processes, in agreement with the luminescence lifetime decays (Table 1).

The addition of dGMP induced major modifications in the transient absorption spectra and the signals decays, as shown in the Figure 5B. Indeed, upon laser flash irradiation, a transient species absorbing in the 390–500 nm region appears and has a lifetime of hundreds of microseconds. This could be explained by a PET from guanine to the excited state of the complex. Indeed, as a result of this photoreaction, a guanine radical and a monoreduced complex Ir(III)-$L^{\bullet-}$ are formed, the latter being responsible for the positive transient absorption. Indeed, the absorption spectrum of the monoreduced complex **1** was measured by spectro-electrochemistry analysis (see Figure S2) and showed a strong absorption band between 390 and 500 nm. On the basis of these results, we can safely conclude that a monoreduced complex is produced upon irradiation in the presence of a guanine unit according to process (eq 1).

$$[Ir(2,2'\text{-}C\text{^}N)_2CPIP]^{3+*} + G \rightarrow [Ir(2,2'\text{-}C\text{^}N^{\bullet-})(2,2'\text{-}C\text{^}N)CPIP]^{2+} + G^{\bullet+} \quad (1)$$

In contrast, we observed a faster decay (330 ns) of the transient absorption band at 450 nm after addition of dAMP (Figure 5C), as compared to the complex alone. Within the concentration ranges of dAMP and complex used, the presence of the monoreduced complex was not observed. This suggests that other processes may occur such as fast back-electron

https://dx.doi.org/10.1021/acs.inorgchem.9b03312
Inorg. Chem. 2020, 59, 2426–2433

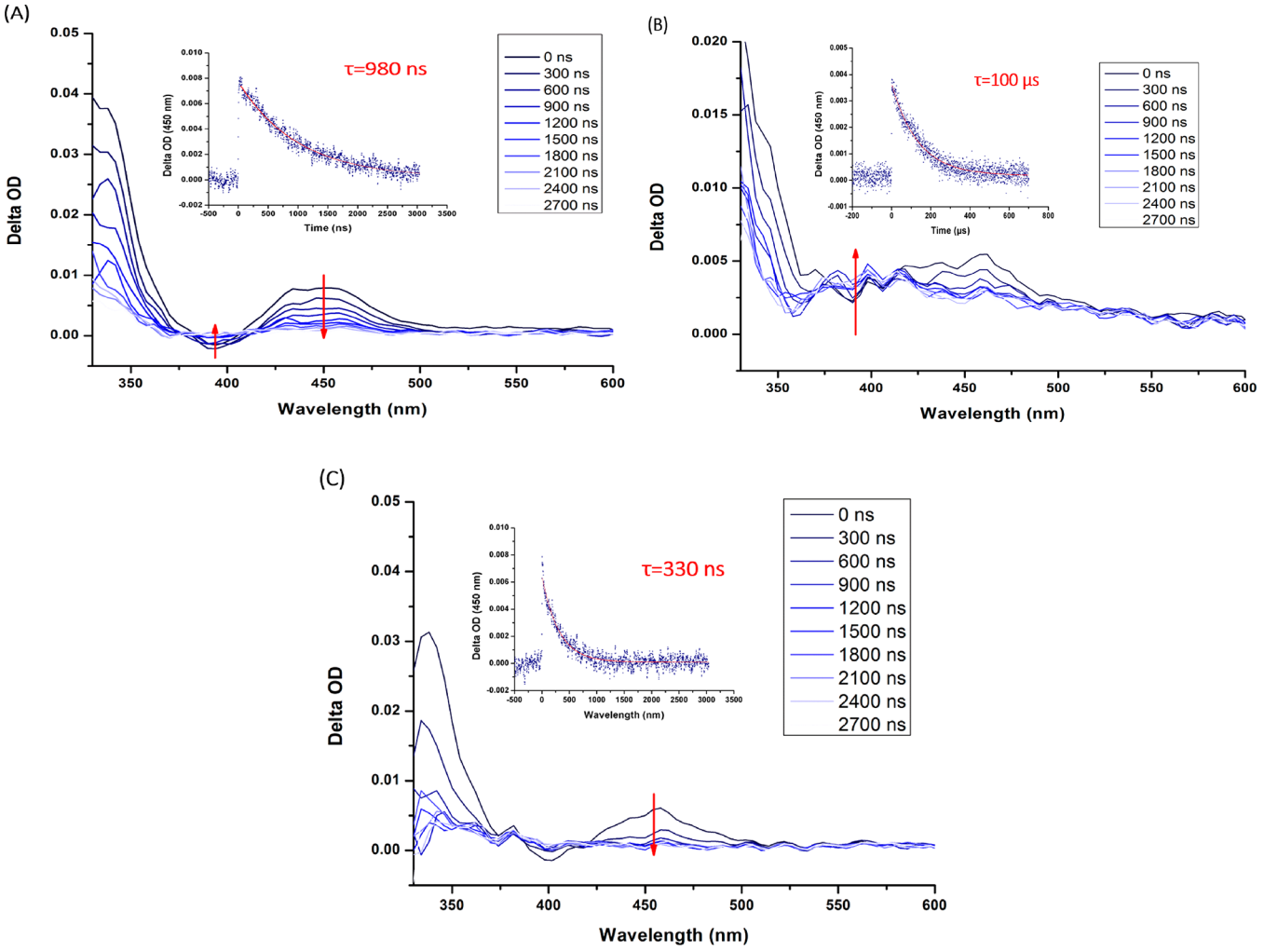

Figure 5. Transient absorption spectra of Ir(III) complex **1** (50 μM) alone (A), as well as in the presence of 10 mM dGMP (B, dGMP/Ir = 20) and 100 mM dAMP (C, dAMP/Ir = 200). Insets: absorbance time profiles at 450 nm. Measurements were performed in deaerated phosphate buffer (10 mM, pH 7.4).

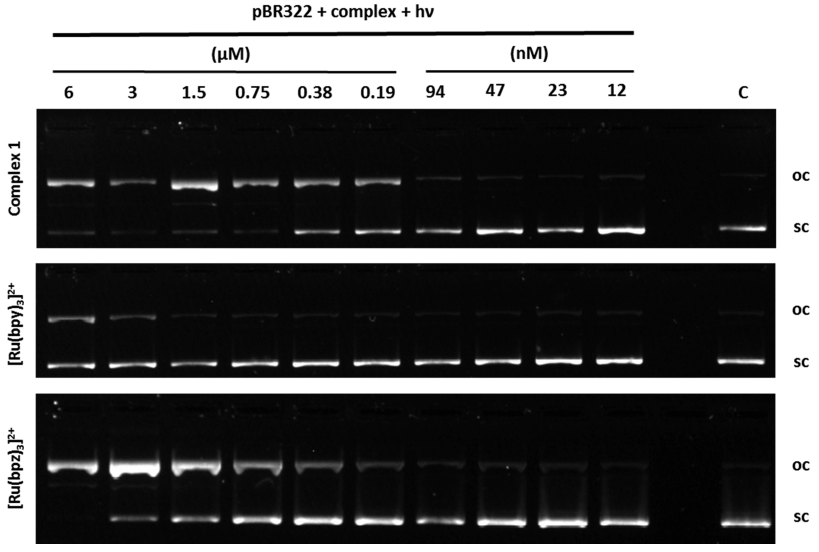

Figure 6. Agarose gel electrophoresis pattern of SC pBR322 DNA. pBR322 plasmid (20 μM) was incubated and irradiated (with blue LED, centered at λ = 405 nm) for 15 min in the presence of different concentrations of complex Ir(III) **1**, $[Ru(bpy)_3]^{2+}$ and $[Ru(bpz)_3]^2$ in Tris-HCl 10 mM (pH 7.2). C, control: pBR322 plasmid incubated for 15 min with the corresponding complex (6 μM) in the dark.

https://dx.doi.org/10.1021/acs.inorgchem.9b03312
Inorg. Chem. 2020, 59, 2426−2433

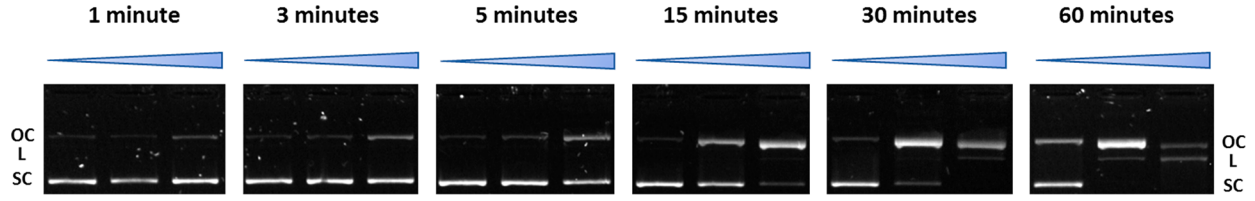

Figure 7. Agarose gel electrophoresis pattern of SC pBR322 (20 μM base pairs) incubated with complex **1** at different concentrations of 20 nM, 200 nM, and 3 μM (respectively from left to right for each irradiation time) and for various irradiation times (1, 3, 5, 15, 30, and 60 min) in Tris-HCl 10 mM (pH 7.2).

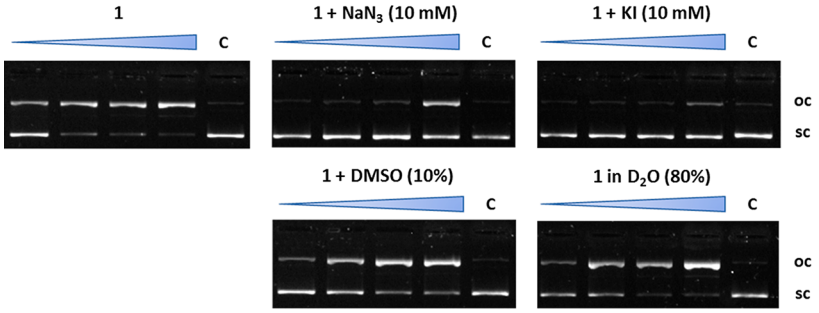

Figure 8. DNA photocleavage reactions in the presence of ROS-specific scavengers or stabilizers. pBR322 (20 μM base pairs) was incubated and irradiated for 15 min with complex **1** concentration of 100 nM, 300 nM, 800 nM, and 6 μM (from left to right for each incubation sample) in Tris-HCl 10 mM (pH 7.2), in the absence of scavengers or stabilizers, in the presence of 10 mM NaN_3, 10 mM KI, 10% DMSO, and 80% D_2O. The control (lanes marked "C") consist of complex **1** (6 μM) + pBR322 plasmid in the dark in the presence of the corresponding scavengers or stabilizers. For the sake of clarity, the control DNA alone and samples with scavengers/stabilizers (in the dark and irradiated) are described in the Supporting Information.

transfer (BET) or photosubstitutions with adenine as previously described for photo-oxidizing Ru(II) complexes, which corroborates the behavior observed for the luminescence titration in the presence of AT-rich hairpin duplex (*vide supra*, Figure 4).[8,32]

DNA Photo-Cleavage. One of the consequences of PET process is the generation of oxidative DNA damages, which could lead to DNA photocleavage. The latter can be easily evidenced by agarose gel electrophoresis using plasmid DNA.[33] pBR322 plasmid DNA is found in a covalently closed circular supercoiled (SC) state, and the formation of oxidative damages may lead to open-circular (OC) and linear (L) isoforms of the plasmid.[33] The formation of OC form arises from a single-strand nick, whereas the L form results from double-strand cleavage. The different isoforms (i.e., SC, OC, and L) can be easily detected on agarose gel electrophoresis due to different electrophoretic mobility. To the best of our knowledge, only a few studies report on the photocleavage process by photo-oxidizing iridium(III) complexes, whereas ruthenium(II) complexes have been the subject of many studies.[6,8,34] In the present case, we investigated the ability of complex **1** to photocleave plasmid DNA and compared its photoactivity to two reference ruthenium(II) complexes, namely, $[Ru(bpy)_3]^{2+}$ (bpy = 2,2′-bipyridine) and $[Ru(bpz)_3]^{2+}$ (bpz = 2,2′-bipyrazine), respectively. $[Ru(bpy)_3]^{2+}$ is known to trigger oxidative damage via singlet oxygen photosensitization (type II photo-oxidation), while $[Ru(bpz)_3]^{2+}$ was shown to undergo a one-electron photoreduction in the presence of a guanine unit (type I photo-oxidation) and to photosensitize $^1O_2$.[34] The coupling of both type I and II processes was shown to significantly increase the conversion of the SC plasmid DNA form into the OC form.[6]

As displayed on Figure 6, after 15 min of light irradiation, complex **1** exhibited a remarkable DNA photocleavage activity as judged by the appearance of the OC isoform at the lowest complex concentration (i.e., 0.19 μM). The formation of the L isoform (i.e., corresponding to a double strand cleavage) was also observed at higher concentration (1.5 μM), whereas in the dark, the same complex at the highest concentration (6 μM) did not show any cleavage activity. Interestingly, the reference complex $[Ru(bpy)_3]^{2+}$ was found to exhibit a moderate photoactivity as the nicked circular OC isoform was formed only in the highest range concentration (3−6 μM). In contrast, $[Ru(bpz)_3]^{2+}$, which can induce both type I and II photo-oxidation, showed similar yields of photocleaved product (i.e., OC isoform) than complex **1**, emphasizing the importance of both processes in the oxidative damages production.

We also examined the DNA photocleavage activity of complex **1** at three different concentrations (20 nM, 200 nM, and 3 μM) as a function of irradiation time (Figure 7). Complex **1** showed dramatic photocleavage activity, since after only 1 min of irradiation and at the highest concentration (i.e., 3 μM) 20% of the SC plasmid was converted already into circular OC form. Furthermore, at this same concentration, more than 90% of cleavage was observed after 1 h of irradiation as it is revealed by the SC form disappearance to the detriment of the formation of 48% of OC (single-strand break) and 52% of L isoforms (double-strand break). Also, at the lowest concentration in complex **1** (i.e., 20 nM), we could still observe the formation of single-strand breaks (15% of OC isoform) after 1 h of irradiation. These results highlight the excellent ability of complex **1** to induce oxidative damages upon irradiation.

DNA Photo-Oxidation with ROS Scavengers and Stabilizers. In order to identify the ROS species possibly involved in the DNA photocleavage, we investigated the photoreactivity profile of **1** in the presence of ROS scavengers (NaN_3: singlet oxygen scavenger; KI: H_2O_2 scavenger; and

https://dx.doi.org/10.1021/acs.inorgchem.9b03312
Inorg. Chem. 2020, 59, 2426−2433

DMSO: OH· scavenger) and stabilizers (D_2O: singlet oxygen stabilizer).[33,35] The scavengers were first confirmed to have no impact on pBR322 in the dark and under light irradiation as shown by agarose gel electrophoresis analysis (see Figure S3). Figure 8 shows that the presence of NaN_3 has a strong effect on the photoreaction. Indeed, the formation of the OC isoform is clearly inhibited (except in the presence of the highest complex concentration, i.e., 6 μM). These results suggest that $^1O_2$ is one of the most prevalent species involved in DNA strand scission through the photoreaction with complex **1**. This is confirmed by using D_2O as $^1O_2$ stabilizer which led to higher cleavage efficiency. It was also noticed that the use of KI as scavenger inhibits the photocleavage ability of **1**, also suggesting the role of H_2O_2 in DNA photo-oxidation.

In contrast, the DNA photodamage was marginally altered by DMSO, suggesting a limited role of the OH· radicals. It is interesting to note that even at high concentration and whatever the scavenger used the cleavage is still operative, suggesting that another photo-oxidative process is still taking place, which can correspond to direct PET with DNA (*vide supra*).

CONCLUSION

In conclusion, we demonstrated herein the ability of the recently described bis-cyclometalated iridium(III) complex, **1**, to trigger PET with guanine and adenine DNA base pairs. These oxidative processes have been characterized and confirmed by electrochemical data, luminescence quenching with mono- and poly nucleotides, and laser flash photolysis. For photoreaction with guanine nucleobase, the study clearly demonstrated a process involving the formation of mono-reduced complex and production of guanine radical cation. The photoreaction with adenine nucleobase turned out to be more complex and likely involves several consecutive steps. Interestingly, the study by agarose gel electrophoresis confirms the ability of the iridium complex to photo-oxidize DNA, by various mechanisms including direct PET with nucleobase, singlet oxygen, and H_2O_2 photoproduction. This study paves the way toward *in cellulo* strategies, for which we expect that our iridium complexes will display remarkable photocytotoxicity, even under hypoxic conditions.

EXPERIMENTAL SECTION

Materials and Methods. $[Ir(2,2'\text{-}C^N)_2CPIP]^{3+}$, complex **1**, was synthesized according to previously described literature protocols.[25] All solvents and reagents for the synthesis were reagent-grade and were used without any further purifications. All solvents for the spectroscopic and electrochemical measurements were of spectroscopic grade. Water was purified with a Millipore Milli-Q system. Agarose, tris-boric acid, and EDTA were purchased from Sigma. Loading buffer (6× loading dye solution) was purchased from Fermentas, and GelRed ×10 000 was from Biotium.

Luminescence Quenching Experiments. dGMP and dAMP titration experiments were recorded on a Varian Cary Eclipse instrument. A solution of dGMP or dAMP (5 mM) was progressively added to a solution of complex **1** (50 μM) in 10 mM Tris-HCl buffer (pH 7.4). Luminescence quenching experiments with ODN (GC- and AT-rich duplex hairpin) were recorded in 10 mM Tris-HCl and 50 mM NaCl (pH 7.4) on a Varian Cary Eclipse instrument. The titration was performed from the highest DNA concentration (10 μM) and progressively decreased, whereas the complex concentration (5 μM) was kept constant.

Transient Absorption Spectroscopy. Transient absorption spectra were acquired using a LP920 K system from Edinburgh Instruments. Excitation was carried out from the third-harmonic (355 nm) of a Brilliant-Quantel Nd:YAG laser at 6 Hz. A Xe900 pulsed Xenon Lamp was used as probe source. The photons were dispersed using a monochromator, transcripted by a R928 (Hamamatsu) photomultiplicator, and recorded on a TDS3012C (Tectronix) oscilloscope.

DNA Cleavage in the Presence of Metal Complexes. Briefly, pBR322 (20 μM base pairs) in 10 mM Tris-HCl (pH 7.2) was incubated in the presence of complex **1**. Reaction mixtures were irradiated with blue light-emitting diode (LED, strip IP68 60 LED/m from Prolumia, 405 nm at 15.7 W/m^2), according to the desired irradiation time, then quenched with DNA loading dye and loaded onto 0.8% agarose gel in Tris-Boric-EDTA buffer (pH 8.2) (0.5× TBE) containing GelRed ×1 (for staining DNA). Electrophoresis was performed at 70 V for 2 h. After DNA migration, the gels were visualized and the fluorescence quantified using Molecular Imager, Gel DocTM XR and image LabTM Software.

DNA Cleavage with ROS Scavengers and Stabilizers. Briefly, pBR322 DNA (20 μM base pairs) in a final volume of 20 μL in 10 mM Tris (pH 7.2) was treated with drug concentrations of 100 nM, 300 nM, 500 nM, and 6 μM in the presence of ROS scavengers/stabilizers: NaN_3 (10 mM), KI (10 mM), DMSO (10%), and D_2O (80%). Reaction mixtures were incubated and irradiated for 15 min, then quenched with DNA loading dye, loaded onto 0.8% agarose gel, and analyzed as described above.

ASSOCIATED CONTENT

Supporting Information

The Supporting Information is available free of charge at https://pubs.acs.org/doi/10.1021/acs.inorgchem.9b03312.

Copy of CD spectra, spectro-electrochemical spectra and control for photocleavage experiments (PDF)

AUTHOR INFORMATION

Corresponding Authors

Eric Defrancq − *Département de Chimie Moléculaire, UMR CNRS 5250, Université Grenoble Alpes, Grenoble 38058, France;* orcid.org/0000-0002-3911-6241; Email: Eric.Defrancq@univ-grenoble-alpes.fr

Benjamin Elias − *Institut de la Matière Condensée et des Nanosciences (IMCN), Molecular Chemistry, Materials and Catalysis Division (MOST), Université catholique de Louvain (UCLouvain), Louvain-la-Neuve B-1348, Belgium;* orcid.org/0000-0001-5037-3313; Email: Benjamin.Elias@uclouvain.be

Authors

Justin Weynand − *Institut de la Matière Condensée et des Nanosciences (IMCN), Molecular Chemistry, Materials and Catalysis Division (MOST), Université catholique de Louvain (UCLouvain), Louvain-la-Neuve B-1348, Belgium; Département de Chimie Moléculaire, UMR CNRS 5250, Université Grenoble Alpes, Grenoble 38058, France;* orcid.org/0000-0003-2104-7601

Angélica Moreno-Betancourt − *Département de Chimie Moléculaire, UMR CNRS 5250, Université Grenoble Alpes, Grenoble 38058, France*

Frédérique Loiseau − *Département de Chimie Moléculaire, UMR CNRS 5250, Université Grenoble Alpes, Grenoble 38058, France;* orcid.org/0000-0003-3648-4863

Nathalie Berthet − *Département de Chimie Moléculaire, UMR CNRS 5250, Université Grenoble Alpes, Grenoble 38058, France*

Complete contact information is available at: https://pubs.acs.org/10.1021/acs.inorgchem.9b03312

https://dx.doi.org/10.1021/acs.inorgchem.9b03312
Inorg. Chem. 2020, 59, 2426−2433

Notes

The authors declare no competing financial interest.

■ ACKNOWLEDGMENTS

This work was supported by the Fonds de la Recherche Scientifique (FNRS) under grant no. J.0091.18. J.W. thanks the "Fonds pour la Formation à la Recherche dans l'Industrie et dans l'Agriculture" (FRIA) and the Erasmus programme for financial support. This work was partially supported by the "Agence National de la Recherche", Labex ARCANE (ANR-16-CE11-0006-01), CBH-EUR-GS (ANR-17-EURE-0003), and the région Auvergne-Rhône-Alpes. The NanoBio-ICMG platforms (FR 2607) are acknowledged for their support. We also thank Dr. Lionel Marcélis for the help with the analysis of the experimental data.

■ REFERENCES

(1) Dasari, S.; Bernard Tchounwou, P. Cisplatin in Cancer Therapy: Molecular Mechanisms of Action. *Eur. J. Pharmacol.* **2014**, *740*, 364−378.

(2) Bergamo, A.; Gaiddon, C.; Schellens, J. H. M.; Beijnen, J. H.; Sava, G. Approaching Tumour Therapy beyond Platinum Drugs: Status of the Art and Perspectives of Ruthenium Drug Candidates. *J. Inorg. Biochem.* **2012**, *106*, 90−99.

(3) Dabrowiak, J. C. Anticancer Agents Beyond Cisplatin. *Metals in Medicine* **2017**, 157−216.

(4) Gill, M. R.; Thomas, J. A. Ruthenium(II) Polypyridyl Complexes and DNA - From Structural Probes to Cellular Imaging and Therapeutics. *Chem. Soc. Rev.* **2012**, *41*, 3179−3192.

(5) Komor, A. C.; Barton, J. K. The Path for Metal Complexes to a DNA Target. *Chem. Commun.* **2013**, *49*, 3617−3630.

(6) Elias, B.; Kirsch-De Mesmaeker, A. Photo-Reduction of Polyazaaromatic Ru(II) Complexes by Biomolecules and Possible Applications. *Coord. Chem. Rev.* **2006**, *250*, 1627−1641.

(7) Uji-i, H.; Foubert, P.; De Schryver, F. C.; De Feyter, S.; Gicquel, E.; Etoc, E.; Moucheron, C.; Kirsch-De Mesmaeker, A. $[Ru(TAP)_3]^{2+}$-Photosensitized DNA Cleavage Studied by Atomic Force Microscopy and Gel Electrophoresis: A Comparative Study. *Chem. - Eur. J.* **2006**, *12*, 758−762.

(8) Lecomte, J.-P.; Kirsch-De Mesmaeker, A.; Feeney, M. M.; Kelly, J. M. Ruthenium(II) Complexes with 1,4,5,8,9,12-Hexaazatriphenylene and 1,4,5,8-Tetraazaphenanthrene Ligands: Key Role Played by the Photoelectron Transfer in DNA Cleavage and Adduct Formation. *Inorg. Chem.* **1995**, *34*, 6481−6491.

(9) Herman, L.; Ghosh, S.; Defrancq, E.; Kirsch-De Mesmaeker, A. Ru(II) Complexes and Light: Molecular Tools for Biomolecules. *J. Phys. Org. Chem.* **2008**, *21*, 670−681.

(10) Pauly, M.; Kayser, I.; Schmitz, M.; Dicato, M.; Del Guerzo, A.; Kolber, I.; Moucheron, C.; Kirsch-De Mesmaeker, A. In vitro Inhibition of Gene Transcription by Novel Photo-activated Polyazaaromatic Ruthenium(II) Complexes. *Chem. Commun.* **2002**, *0*, 1086−1087.

(11) Archer, S. A.; Raza, A.; Dröge, F.; Robertson, C.; Auty, A. J.; Chekulaev, D.; Weinstein, J. A.; Keane, T.; Meijer, A. J. H. M.; Haycock, J. W.; MacNeil, S.; Thomas, J. A. A Dinuclear Ruthenium-(II) Phototherapeutic that Targets Duplex and Quadruplex DNA. *Chem. Sci.* **2019**, *10*, 3502−3513.

(12) Marcélis, L.; Kajouj, S.; Ghesquière, J.; Fettweis, G.; Coupienne, I.; Lartia, R.; Surin, M.; Defrancq, E.; Piette, J.; Moucheron, C.; Kirsch-De Mesmaeker, A. Highly DNA-Photoreactive Ruthenium 1,4,5,8- Tetraazaphenanthrene Complex Conjugated to the TAT Peptide: Efficient Vectorization inside HeLa Cells without Phototoxicity - The Importance of Cellular Distribution. *Eur. J. Inorg. Chem.* **2016**, *2016*, 2902−2911.

(13) Kajouj, S.; Marcélis, L.; Lemaur, V.; Beljonne, D.; Moucheron, C. Photochemistry of Ruthenium(II) Complexes based on 1,4,5,8-Tetraazaphenanthrene and 2,2'-Bipyrazine: a Comprehensive Experimental and Theoretical Study. *Dalton Trans.* **2017**, *46*, 6623−6633.

(14) Hess, J.; Huang, H.; Kaiser, A.; Pierroz, V.; Blacque, O.; Chao, H.; Gasser, G. Evaluation of the Medicinal Potential of Two Ruthenium(II) Polypyridine Complexes as One- and Two-Photon Photodynamic Therapy Photosensitizers. *Chem. - Eur. J.* **2017**, *23*, 9888−9896.

(15) Liu, B.; Monro, S.; Lystrom, L.; Cameron, C. G.; Colón, K.; Yin, H.; Kilina, S.; McFarland, S. A.; Sun, W. Photophysical and Photobiological Properties of Dinuclear Iridium(III) Bis-tridentate Complexes. *Inorg. Chem.* **2018**, *57*, 9859−9872.

(16) Bevernaegie, R.; Marcélis, L.; Laramée-Milette, B.; De Winter, J.; Robeyns, K.; Gerbaux, P.; Hanan, G. S.; Elias, B. Trifluoromethyl-Substituted Iridium(III) Complexes: From Photophysics to Photooxidation of a Biological Target. *Inorg. Chem.* **2018**, *57*, 1356−1367.

(17) Jacques, A.; Kirsch-De Mesmaeker, A.; Elias, B. Selective DNA Purine Base Photooxidation by Bis-terdentate Iridium(III) Polypyridyl and Cyclometalated Complexes. *Inorg. Chem.* **2014**, *53*, 1507−1512.

(18) Huang, H.; Banerjee, S.; Sadler, P. J. Recent Advances in the Design of Targeted Iridium(III) Photosensitizers for Photodynamic Therapy. *ChemBioChem* **2018**, *19*, 1574−1589.

(19) Pracharova, J.; Vigueras, G.; Novohradsky, V.; Cutillas, N.; Janiak, C.; Kostrhunova, H.; Kasparkova, J.; Ruiz, J.; Brabec, V. Exploring the Effect of Polypyridyl Ligands on the Anticancer Activity of Phosphorescent Iridium(III) Complexes: From Proteosynthesis Inhibitors to Photodynamic Therapy Agents. *Chem. - Eur. J.* **2018**, *24*, 4607−4619.

(20) Shao, F.; Elias, B.; Lu, W.; Barton, J. K. Synthesis and Characterization of Iridium(III) Cyclometalated Complexes with Oligonucleotides: Insights into Redox Reactions with DNA. *Inorg. Chem.* **2007**, *46*, 10187−10199.

(21) Nakagawa, A.; Hisamatsu, Y.; Moromizato, S.; Kohno, M.; Aoki, S. Synthesis and Photochemical Properties of pH Responsive Tris-Cyclometalated Iridium(III) Complexes That Contain a Pyridine Ring on the 2-Phenylpyridine Ligand. *Inorg. Chem.* **2014**, *53*, 409−422.

(22) Kando, A.; Hisamatsu, Y.; Ohwada, H.; Itoh, T.; Moromizato, S.; Kohno, M.; Aoki, S. Photochemical Properties of Red-Emitting Tris(cyclometalated) Iridium(III) Complexes Having Basic and Nitro Groups and Application to pH Sensing and Photoinduced Cell Death. *Inorg. Chem.* **2015**, *54*, 5342−5357.

(23) He, L.; Li, Y.; Tan, C.-P.; Ye, R.-R.; Chen, M.-H.; Cao, J.-J.; Ji, L.-N.; Mao, Z.-W. Cyclometalated Iridium(III) Complexes as Lysosometargeted Photodynamic Anticancer and Real-Time Tracking Agents. *Chem. Sci.* **2015**, *6*, 5409−5418.

(24) Tian, X.; Zhu, Y.; Zhang, M.; Luo, L.; Wu, J.; Zhou, H.; Guan, L.; Battaglia, G.; Tian, Y. Localization Matters: a Nuclear Targeting two-Photon Absorption Iridium Complex in Photodynamic Therapy. *Chem. Commun.* **2017**, *53*, 3303−3306.

(25) Weynand, J.; Bonnet, H.; Loiseau, F.; Ravanat, J.-L.; Dejeu, J.; Defrancq, E.; Elias, B. Targeting G-rich DNA Structures with Photo-Reactive bis-Cyclometalated Iridium(III) Complexes. *Chem. - Eur. J.* **2019**, *25*, 12730−12739.

(26) Castor, K. J.; Liu, Z.; Fakhoury, J.; Hancock, M. A.; Mittermaier, A.; Moitessier, N.; Sleiman, H. F. A Platinum(II) Phenylphenanthroimidazole with an Extended Side-Chain Exhibits Slow Dissociation from a c-Kit G-Quadruplex Motif. *Chem. - Eur. J.* **2013**, *19*, 17836−17845.

(27) Castor, K. J.; Metera, K. L.; Tefashe, U. M.; Serpell, C. J.; Mauzeroll, J.; Sleiman, H. F. Cyclometalated Iridium(III) Imidazole Phenanthroline Complexes as Luminescent and Electrochemiluminescent G-Quadruplex DNA Binders. *Inorg. Chem.* **2015**, *54*, 6958−6967.

(28) Weynand, J.; Diman, A.; Abraham, M.; Marcélis, L.; Jamet, H.; Decottignies, A.; Dejeu, J.; Defrancq, E.; Elias, B. Towards the Development of Photo-Reactive Ruthenium (II) Complexes Targeting Telomeric G-quadruplex DNA. *Chem. - Eur. J.* **2018**, *24*, 19216−19227.

https://dx.doi.org/10.1021/acs.inorgchem.9b03312
Inorg. Chem. 2020, 59, 2426−2433

(29) Steenken, S.; Jovanovic, S. V. How Easily Oxidizable Is DNA? One-Electron Reduction Potentials of Adenosine and Guanosine Radicals in Aqueous Solution. *J. Am. Chem. Soc.* **1997**, *119*, 617−618.
(30) Rehm, D.; Weller, A. Kinetics of Fluorescence Quenching by Electron and H-Atom Transfer. *Isr. J. Chem.* **1970**, *8*, 259−271.
(31) Bevernaegie, R.; Marcélis, L.; Moreno-Betancourt, A.; Laramée-Milette, B.; Hanan, G. S.; Loiseau, F.; Sliwa, M.; Elias, B. Ultrafast Charge Transfer Excited State Dynamics in Trifluoromethyl-Substituted Iridium(III) Complexes. *Phys. Chem. Chem. Phys.* **2018**, *20*, 27256−27260.
(32) Lecomte, J. P.; Kirsch-De Mesmaeker, A.; Kelly, J. M. Photochemistry of Ruthenium(II)-Tris-1,4,5,8-Tetraazaphenanthrene with Mononucleotides: Role of Ligand Photosubstitution. *Bull. Soc. Chim. Belg.* **1994**, *103*, 193−200.
(33) Kellett, A.; Molphy, Z.; Slator, C.; McKee, V.; Farrell, N. P. Molecular Methods for Assessment of non-Covalent Metallodrug-DNA Interactions. *Chem. Soc. Rev.* **2019**, *48*, 971−988.
(34) Vicendo, P.; Mouysset, S.; Paillous, N. Comparative Study of $Ru(bpz)_3^{2+}$ $Ru(bipy)_3^{2+}$ and $Ru(bpz)_2CI_2$ as Photosensitizers of DNA Cleavage and Adduct Formation. *Photochem. Photobiol.* **1997**, *65*, 647−655.
(35) Slator, C.; Barron, N.; Howe, O.; Kellett, A. [Cu(o-phthalate)(phenanthroline)] Exhibits Unique Superoxide-Mediated NCI-60 Chemotherapeutic Action through Genomic DNA Damage and Mitochondrial Dysfunction. *ACS Chem. Biol.* **2016**, *11*, 159−171.

https://dx.doi.org/10.1021/acs.inorgchem.9b03312
Inorg. Chem. 2020, 59, 2426−2433